SPACE TELESCOPE SCIENCE INSTITUTE
Operated for NASA by AURA

**Instrument Science Report WFC3 2007-23**

# WFC3 TV2 Testing: IR Channel Throughput

Thomas M. Brown
Oct 23, 2007

**ABSTRACT**

*A new IR detector (IR1; FPA129) was housed in WFC3 during the most recent campaign of thermal vaccum (TV) ground testing at GSFC. We performed measurements of the IR channel throughput over the course of ground testing, and found that the throughput is near expectations on the blue end of the IR channel wavelength range, but approximately 20% lower than expectations on the red end. This is in contrast to the results of the first WFC3 TV tests in 2004, when the previous IR detector (IR2; FPA064) was in the instrument; there, we found a grey deficiency of 15% in the measured throughput.*

*The throughput measurements in the current campaign were repeated many times, with many variations on the test procedure, to understand the strong variations in the calculated throughput. In the end, these variations were traced to an instability in the optical stimulus used for these tests, not the WFC3 optics or detector. Unfortunately, this problem means that all of the IR1 images in the archive record an erroneous value for the optical stimulus flux. Most of these records cannot be corrected, due to the unknown state of the optical stimulus at the time the data were obtained, but the final two throughput tests were performed in tandem with a calibration of the optical stimulus that accounted for these systematic errors; the correction from this contemporaneous calibration has been applied here.*

## Background

The Wide Field Camera 3 (WFC3) recently underwent ground testing under thermal vacuum (TV) conditions. A new IR detector (IR1; FPA129) is currently installed in the instrument, replacing the detector in use during the 2004 TV tests (IR2; FPA064). The new detector has been substrate thinned in order to mitigate a potential issue with these detectors, wherein they produce

elevated dark rates in response to cosmic ray impacts; this thinning process also enhances the quantum efficiency (QE) of the detector, particularly at blue wavelengths.

Among the tests performed in TV is a measurement of the end-to-end throughput (i.e., the throughput of the entire instrument excluding the HST OTA). The current tests are very similar to the tests performed during the first TV campaign (see Brown et al. 2005, ISR WFC3 2005-12 for details). On the UVIS channel, throughput measurements are made with no WFC3 filter in the beam (i.e., "CLEAR" mode; see Brown 2007, ISR WFC3 2007-20), but there is no corresponding CLEAR mode on the IR channel; all measurements are made with one of the 15 IR channel filters in the beam.

## Test Setup

For the IR throughput tests, WFC3 was illuminated with an optical stimulus (called "CASTLE") that can deliver flux-calibrated monochromatic light to the WFC3 focal plane. We employed the 200 micron fiber on CASTLE, fed by a Tungsten lamp in combination with a double monochromator, producing a spot approximately 6 pixels across on the WFC3 IR detector. This large spot allows the throughput to be measured more accurately, because it averages over pixel-to-pixel variation in response and allows a large number of counts in the measurement (generally >> 10,000 electrons) without approaching the saturation limit of the IR detector (~100,000 electrons per pixel). For the nominal throughput tests in the TV campaign (SMS IR11S11A), the CASTLE bandpass was set to 5 nm, the CASTLE monochromator wavelength was set to a point near the center of the WFC3 bandpass of each filer, the CASTLE ND filter was set to ND5 (which is actually two filters: ND4+ND1), and WFC3 was read in RAPID full-frame mode. The first two tests were run with SMS IR11S11, which used the name of the filter to drive the wavelength specified for each filter, but this was not sufficiently centered in the narrow-band filters, so the revised test (SMS IR11S11A) tweaked the wavelengths for the narrow-band filters (e.g., F167N was changed from 1670 nm to 1666 nm). On the last day of TV (11 Oct 2007), we also ran a variation (SMS IR11S32) of the nominal test that sampled a more regular wavelength grid through three broadband WFC3 filters, employed a 10 nm CASTLE bandpass, an ND4 filter setting on CASTLE, and a 512x512 subarray RAPID read sequence (to accommodate the brighter CASTLE illumination seen through ND4 instead of ND5).

CASTLE provides a photon flux using its own reference detectors, employing a Si photodiode at 1 micron and bluer wavelengths (the same reference detector used at the red end of the UVIS throughput tests), and an InGaAs photodiode at wavelengths above 1 micron. These reference detectors are far less sensitive than the WFC3 IR detector; thus, ND filters are inserted in the beam when illuminating WFC3, and removed from the beam when illuminating the CASTLE reference detectors. The WFC3 IR throughput measurements thus depend upon a calibration of these ND filters. The measured throughput is simply the count rate observed on WFC3 (electrons per second) divided by the flux measured by CASTLE (photons per second), with the latter appropriately normalized to account for the ND filter transmission. The WFC3 UVIS throughput measurements on the red end of the UVIS range are done in a similar manner, but employ ND3 and ND2 filters on CASTLE and a 10 nm bandpass.

For the tests described herein, the commanded gain was 2.0, resulting in an actual gain of 2.42, 2.44, 2.41, and 2.46 in quadrants 1, 2, 3, and 4, respectively (B. Hilbert, private communication). The numbering convention for the quadrants assumes quad 1 is in the upper left-hand corner, and that the quadrants increase as one moves counter-clockwise from quad 1. Hilbert's gain calculations did not correct for the interpixel capacitance (IPC), which would scale the gain by 0.88 (B. Hill, private communication), but that correction has been applied in this analysis. Almost all of the throughput measurements in the recent TV campaign were made with the CASTLE spot in quad 3, and so a gain of 2.41x0.88=2.12 is used here.

Another factor worth noting is the flat-field, which has a fair amount of structure due to thinning of the detector substrate. Inspection of IR flats taken in a variety of filters with both external and internal illumination implies that there is nothing particularly unusual about the location of the illumination spot during the TV tests. Ratios of flats show spots a few pixels across, likely due to dust motes on the channel select mechanism (CSM) in combination with small drifts in the CSM between images, but none of these spots fall near the location used for throughput measurements. These flat ratios also show larger spots (tens of pixels in diameter) and a "window frame" where the flats vary at the ~2% level, perhaps due to condensation on the IR detector window, but again, none of these structures falls in a location that would affect the throughput measurements. The throughput field point (called IR01) appears representative of the detector.

The WFC3 images were processed with a minimal IDL-based pipeline that fits and subtracts the signal in the appropriate reference pixels (using 4 of the reference pixel columns along the left and right sides of the image), fits a line to counts vs. time in the non-destructive read sequence for each pixel in an exposure, and scales by the gain. Although some of the hot pixels exhibit extremely non-linear behavior, the pixels within the CASTLE illumination spot were linear over the full read sequence to ~1% or better. Dark images taken with the same read sequence and contemporaneous with each throughput exposure were processed with the same pipeline and then subtracted from the corresponding throughput image.

For most of the throughput tests acquiring a full wavelength sweep, we ran a companion test that obtained the same alternating sequence of filtered throughput, dark, filtered throughput, dark, etc., but with the CASTLE monochromator shuttered and the CASTLE lamp turned off; SMS IR11S21 was the companion to IR11S11A, while IR11S42 was the companion to IR11S32. This companion test provided a measurement of the light leak in the CASTLE fiber, which would result in detected counts for WFC3 but would not be included in the CASTLE flux calibration (since it is chopped). The dark-subtracted images from the companion test were subtracted from the dark-subtracted images in the throughput run, thus correcting for the faint light leak in the CASTLE fibers; this correction has a discernible effect at the 1% level for the blue end of the IR channel wavelength range, and is negligible for the red end. There was no companion test to the first two throughput runs (IR11S11), and the CASTLE fibers were not well-wrapped until the second throughput run, but these runs (and many others) are not actually included in the analysis reported here. The resulting images were then subjected to aperture photometry using an aperture radius of 20 and a sky annulus of radii 20 to 30 pixels, providing a measure of the count rate detected by WFC3. The photometry thus has three levels of background subtraction (contemporaneous dark, companion images with CASTLE source shuttered,

and sky annulus), with all of these corrections being extremely small, given the relatively high count rate in the source itself. The throughput is then the ratio of the detector count rate (electrons/second) to the CASTLE-provided measurement of the incoming flux (photons/second), where the CASTLE flux is recorded in the "OSFLUX" header keyword.

## Investigation of Throughput Variability

For much of the TV campaign, the IR throughput appeared to be varying in a wavelength-dependent manner by as much as 20% on timescales of days to weeks and 3% on the timescales of hours to days. The throughput test was repeated many times to track this issue, with variations on the standard test to try and isolate the cause. Some of this investigation involved the comparison of tests performed before and after warmup of the instrument (during side changes on the instrument electronics, chamber breaks, and intentional bake-outs), but the throughput did not consistently respond to these warmups. Theories ranged from contamination (given the cold optics and detector), coating degradation, detector instability, CASTLE calibration issues, data analysis issues, etc.

In the end, it turned out that the problem was an instability in the CASTLE. When CASTLE steers the beam onto the WFC3 pickoff mirror (POM), a distorted image of the monochromator slit is projected onto a target fiber (Figure 1; R. Telfer, private communication). The image of the slit looks like a crescent moon, with a width dependent upon the slit width (which is a function of the chosen bandpass). As stated in the previous section, CASTLE records a flux on its reference detectors to provide flux calibration during a throughput test, but the ND filters needed for the WFC3/IR exposure are removed from the beam during the CASTLE flux calibration, since the CASTLE reference detectors are less sensitive than WFC3. Thus, the flux calibration depends upon the ND calibration; this ND calibration was repeated during CASTLE down time, typically every few weeks. Near the end of the TV campaign, the CASTLE operators noted that the ND calibration was done with a bandpass of 13 nm instead of the 5 nm used for the standard WFC3/IR throughput tests, in order to improve the signal-to-noise ratio in the ND calibration. That wider bandpass corresponds to a wider monochromator slit and thus a wider slit image falling on the target fiber. Repeated calibrations of the CASTLE ND transmission showed much more stability than the throughput tests, but this was because the wider slit image did not suffer from alignment problems with the fiber. Then, when a 5 nm bandpass was used in the throughput tests, the narrower slit image illuminated the fiber in a way that was particularly sensitive to fiber stage alignment. In addition, the act of inserting and removing ND filters from the beam shifted the slit image with respect to the target fiber, and this variation was a significant source of instability when the slit image was narrow (as in the 5 nm WFC3 throughput run).

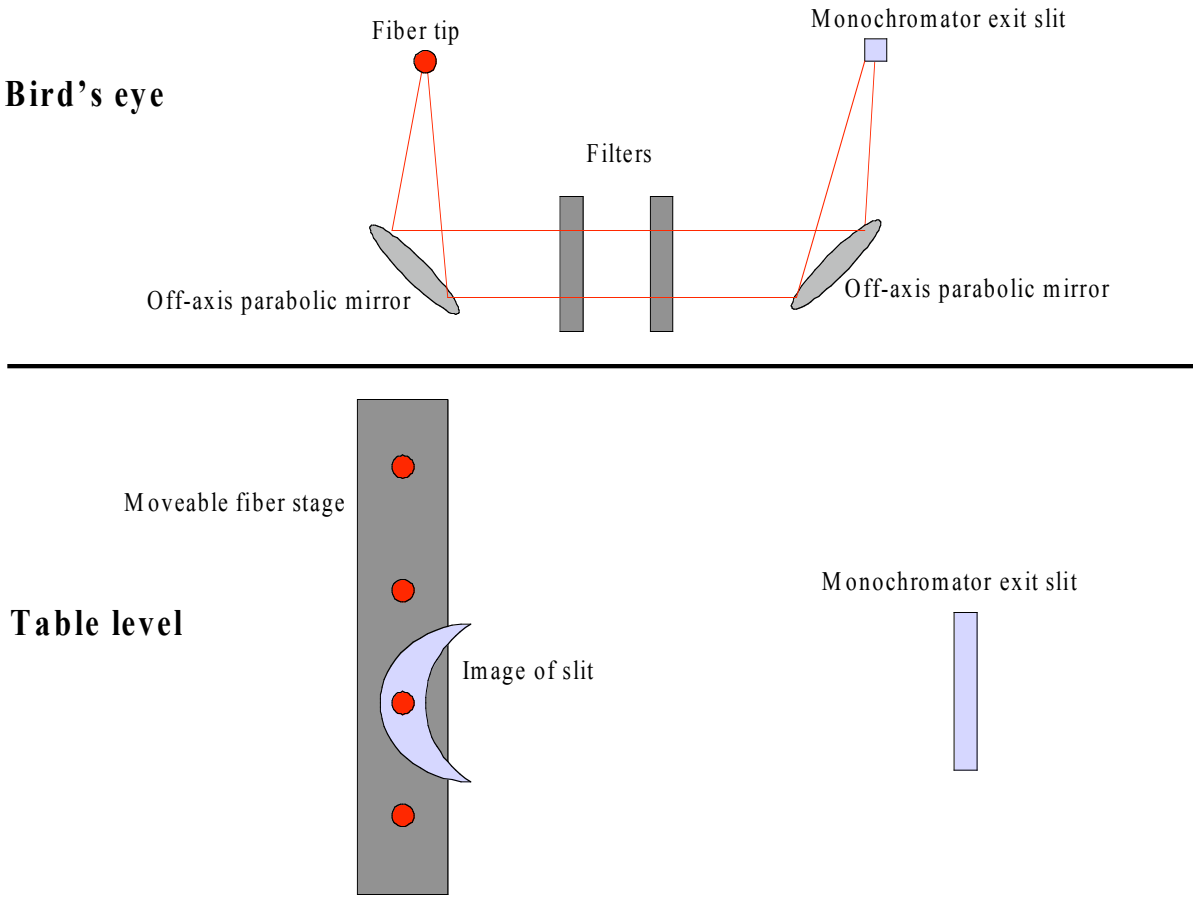


Figure 1: A schematic showing the illumination of the target fiber stage within CASTLE (courtesy R. Telfer, private communication).

The varying illumination of the CASTLE fiber in the WFC3 throughput tests was likely due to a variety of instabilities that affect the position of the monochromator slit image with respect to the target fiber position (wedge in the ND filters, fiber stage motion, lamp alignment, etc.). We investigated the effect of these alignment instabilities by performing throughput measurements at 4 wavelengths (910 nm / F110W, 1100 nm / F110W, 1400 nm /F140W, and 1600 nm / F160W) with a variety of CASTLE fiber stage positions (Figure 2), commanding the CASTLE fiber stage to move in the Y direction (it cannot be commanded in X, which would yield even more variation with position, given the shape of the slit image). As we scanned the CASTLE fiber stage position, the relative throughput measured by the test varied significantly at all wavelengths (-5%/+15% relative to the start of the test), with significant wavelength dependence in the vicinity of the "nominal" fiber stage position, where most of the tests were performed during the TV campaign. The last two throughput runs of TV were done at a "good" position, where the throughput was varying fairly slowly with fiber stage position in a manner largely independent of wavelength. This fiber stage position was also calibrated on the same day, providing an accurate

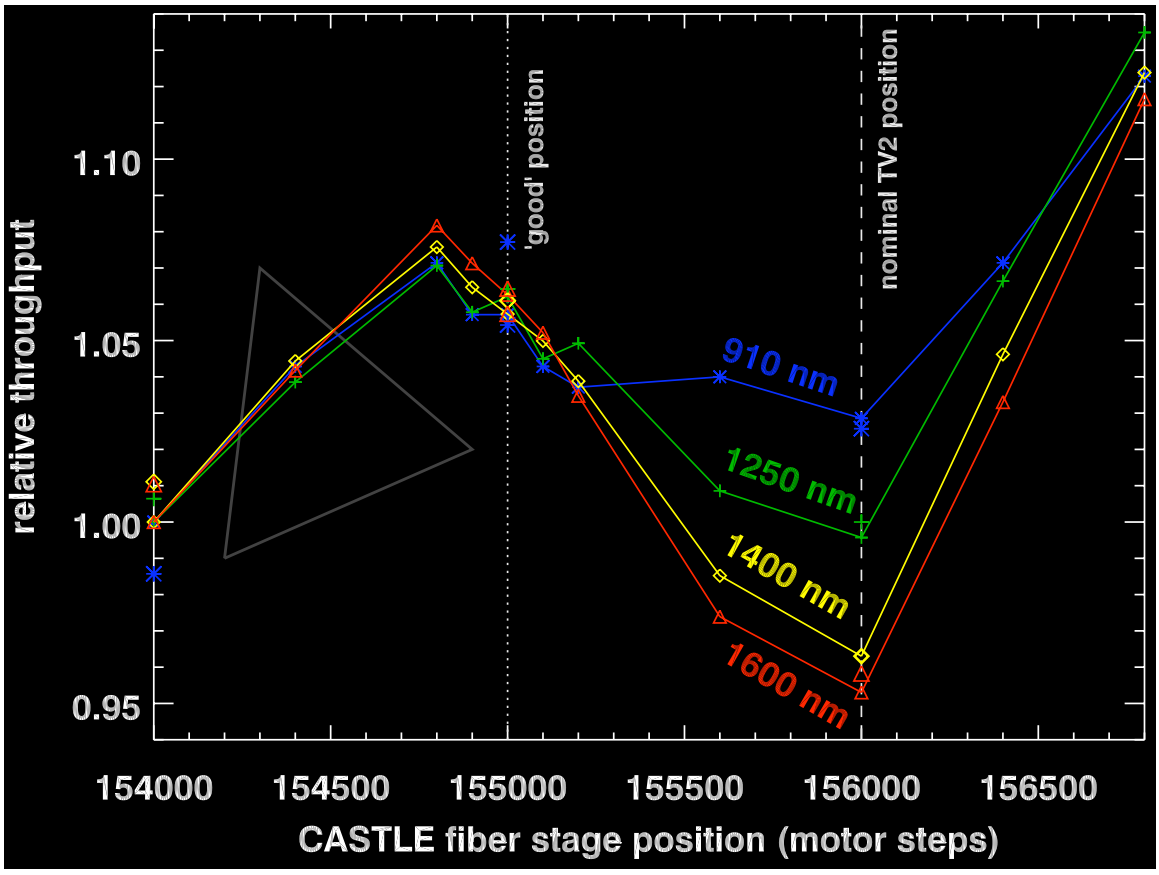


Figure 2: Relative throughput calculated from the measurements at 4 wavelengths, as a function of CASTLE fiber stage position in one axis. The fiber stage was near the dashed line during most of TV, but the last two throughput tests were done at the dotted line.

CASTLE flux measurement (a correction to the flux in the image header), which in turn enables an accurate throughput measurement.

During the investigation of the throughput anomaly, many iterations of the throughput test were executed. Given the current understanding of the problem, it would be moot to report on most of those tests, since the CASTLE fiber stage alignment was in an unknown state for them. However, it is worth noting a few variations of the test here, because absolute throughput aside, they give confidence in the instrument performance in a variety of configurations.

One test (IR11S18) performed throughput measurements in F160W in a rapid sequence: F160W w/flux calibration, dark, F160W, F160W, F160W, dark, F160W, F160W, F160W, dark, F160W, F160W, F160W, dark, F160W w/flux calibration, F160W, F160W, F160W, dark, F160W, F160W, F160W, dark, F160W, F160W, F160W, dark, F160W w/flux calibration. The point here was to monitor the CASTLE flux at only 3 points (the beginning, middle, and end of the test), to minimize configuration changes on CASTLE. During the last run of this test, when the instrument and CASTLE were in a stable configuration, the count rate measured by WFC3 had an r.m.s. of 0.2% in the full run of 18 images, demonstrating the ability of WFC3 to obtain stable photometry.

Another test obtained throughput measurements at 4 wavelengths (980 nm / F980M, 1250 nm / F125W, 1400 nm /F140W, and 1600 nm /F160W), saturated with blue light at the 100x level (using the F098M filter), obtained two more sets of throughput measurements (at the same 4 wavelengths), saturated with red light at the 100x level (using the F160W filter), and then obtained two more sets of throughput measurements. The point here was to look for hysteresis effects. The r.m.s. in the count rate for each filter varied from 1-2%, consistent with the scatter one would expect from manipulating the CASTLE between exposures, and thus giving no indication of a hysteresis problem.

Yet another test obtained throughput measurements at these same four combinations of wavelength and filter, but repeated them in subarrays: 1024x1024 w/ND5, 512x512 w/ND5, 256x256 w/ND4, and 128x128 w/ND4. At 980 nm, the 1024x1024 count rate agreed with the 512x512 count rate to better than 1%, while the 256x256 count rate agreed with the 128x128 count rate to 4%. At 1250 and 1400 nm, the 1024x1024 count rate agreed with the 512x512 count rate at the level of 2-3%, while the 256x256 count rate agreed with the 128x128 count rate at the level of 1%. At 1600 nm, the 1024x1024 vs. 512x512 and 256x256 vs. 128x128 comparisons were both in agreement at the 3% level. None of these comparisons indicated any systematic offsets due to changing the size of the frame, and the scatter is typical for a series of images acquired with CASTLE flux calibrations.

Two runs of a cross-check between the UVIS and IR channels were performed near the end of the TV campaign (SMS IR11S19). This test obtains a throughput measurement in the UVIS/CLEAR and the IR/F098M configurations on WFC3, with CASTLE set to the nominal IR throughput field point, 980 nm with a 10 nm bandpass, and the ND5 filter. The CASTLE fiber stage was moved between the two tests, with neither fiber stage position at the “good” position shown in Figure 2. The two runs of the test show a 12% change in the calculated throughput on the UVIS channel, if taken at face value. However, we already know the UVIS throughput is extremely stable (Brown 2007, ISR WFC3 2007-20). If we normalize the UVIS throughputs at each fiber stage position to the nominal UVIS throughput at this wavelength (interpolating the results at 950 nm and 1000 nm in Brown 2007, ISR WFC3 2007-20), then apply the same normalization factors to the IR throughput measurements, the corrected IR throughput measurements differ by only 1.6%, and agree at the 1-3% level with the F098W throughput measurement obtained on the last day of TV (described below).

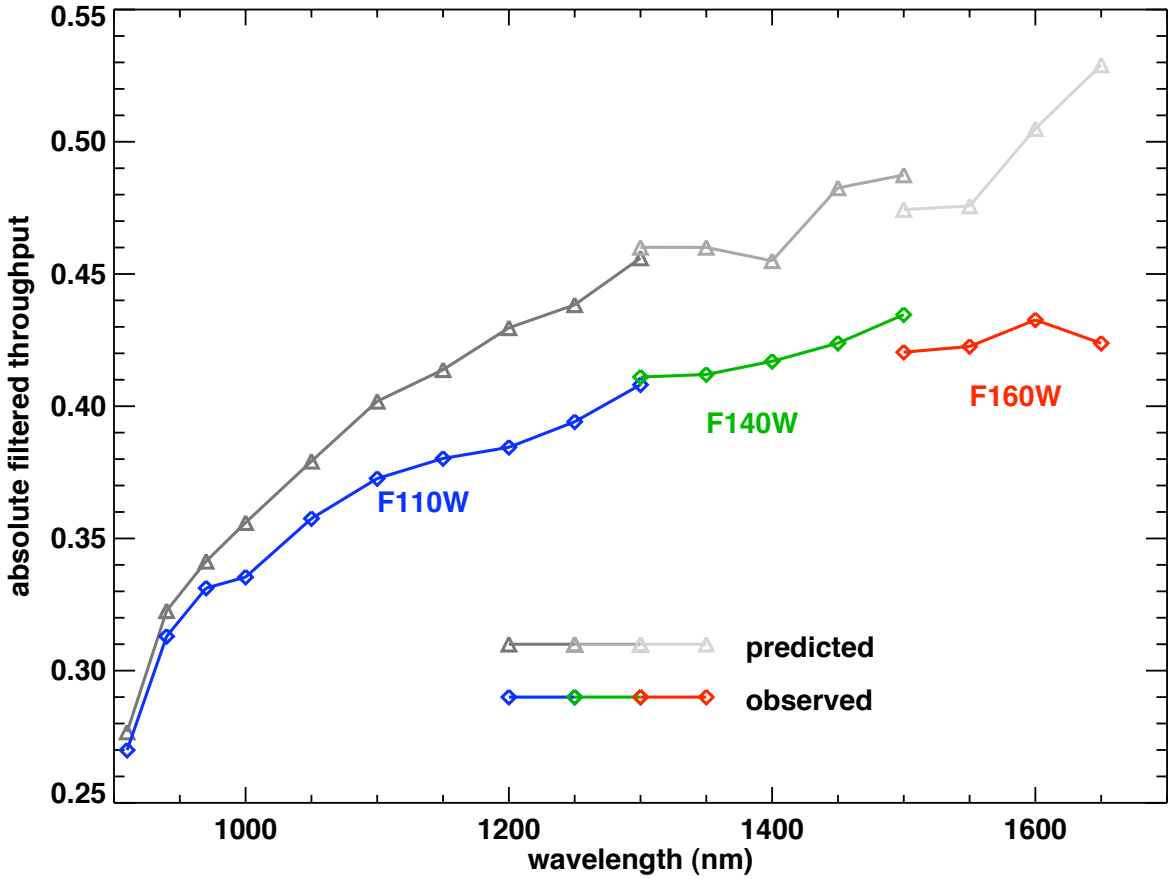


Figure 3: The IR throughput measurements resulting from SMS IR11S20 on the last day of TV (*colored lines*) compared to the throughput expected from the product of the component measurements (*grey lines*). The throughputs shown above include the IPC correction in both the observed and predicted values.

## Results

On the last day of TV, two throughput runs were obtained. The first (IR11S32) obtained a regular wavelength grid in three WFC3 filters (F110W, F140W, and F160W) using a 512x512 subarray, with CASTLE employing a 10 nm bandpass, the ND4 filter, and the "good" fiber stage position, thus minimizing sensitivity to CASTLE alignment issues. This test was followed by its companion test (IR11S42), with the CASTLE shuttered. The second test (IR11S11A) checked one wavelength for each of the 15 WFC3 filters using a 1024x1024 full-frame image, with CASTLE employing a 5 nm bandpass, the ND5 filter, and the "good" fiber stage position; the 5 nm bandpass makes the test susceptible to alignment issues on CASTLE, but a CASTLE calibration was done the same day for both ND5 and ND4, using the same configuration employed in these WFC3 tests, hoping to minimize any systematic errors. This test was also followed by its

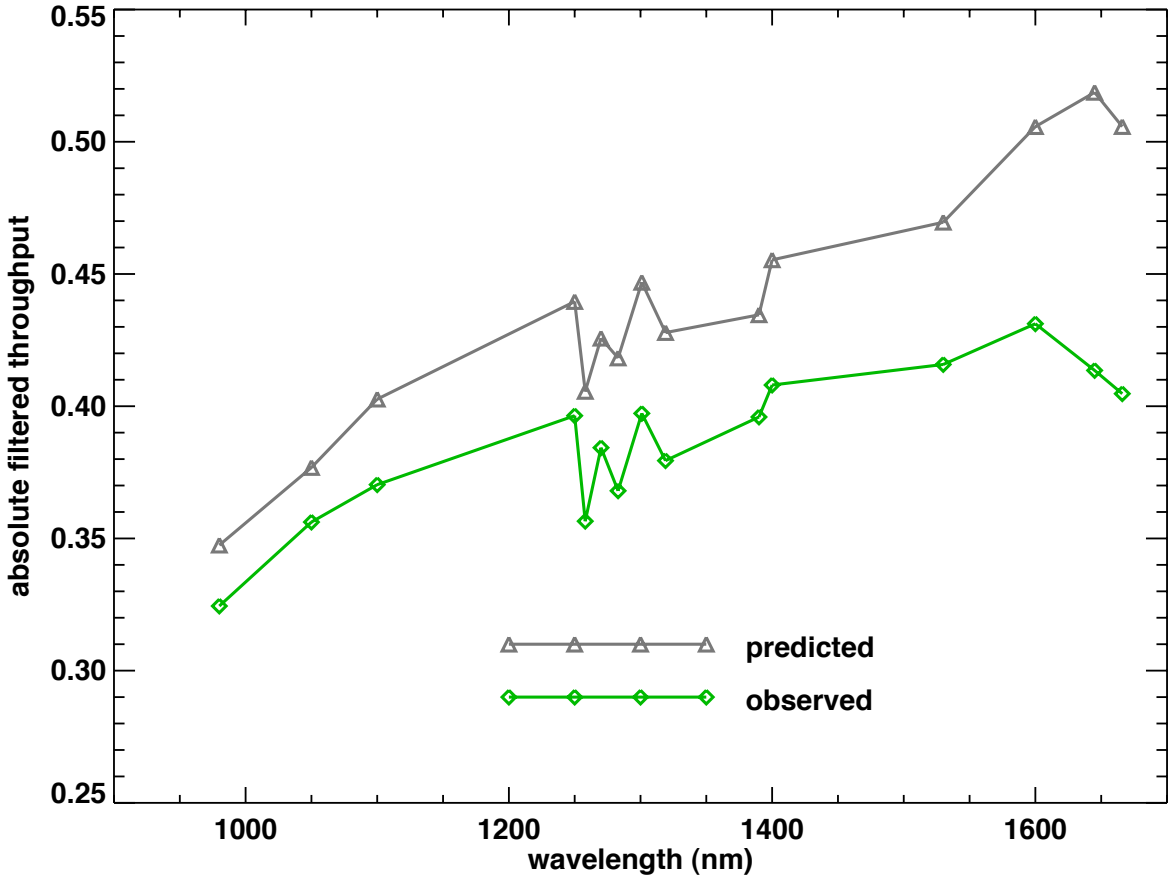


Figure 4: The same as in Figure 3, but for SMS IR11S11A, which obtains a throughput measurement in each filter of the IR channel.

companion test (IR11S21), with the CASTLE shuttered. Fortunately, the two tests agree very well, as shown in Figures 3 and 4 and Tables 1 and 2. If taken at face value, each test finds good agreement with the expected throughput of the instrument (based upon the product of the component throughputs) at the blue end of the IR channel wavelength range, with increasing deficiency in throughput as one moves to the red, culminating at a 20% deficiency. These results are not the same as those found for the first IR detector, in the 2004 TV campaign (Brown et al. 2005, ISR WFC3 2005-12), where there was a wavelength-independent throughput deficit of ~15%., stable over the course of that TV campaign. The cause of the deficiency in each TV campaign remains unexplained. Unfortunately, we can at this time provide no throughput trend vs. time in the most recent TV campaign, given the systematic errors in the measurements prior to the last day of the test.

Table 1: Throughput results for IR11S32

| wavelength (nm) | filter | observed count rate ($e^-$/sec) | measured throughput | expected throughput | measured to expected |
|---|---|---|---|---|---|
| 910 | F110W | 10500 | 0.270 | 0.277 | 0.975 |
| 940 | F110W | 20325 | 0.313 | 0.323 | 0.970 |
| 970 | F110W | 37808 | 0.331 | 0.341 | 0.969 |
| 1000 | F110W | 61159 | 0.335 | 0.356 | 0.941 |
| 1050 | F110W | 113450 | 0.357 | 0.379 | 0.942 |
| 1100 | F110W | 162774 | 0.372 | 0.402 | 0.926 |
| 1150 | F110W | 206698 | 0.380 | 0.414 | 0.919 |
| 1200 | F110W | 241394 | 0.385 | 0.429 | 0.895 |
| 1250 | F110W | 257516 | 0.394 | 0.438 | 0.900 |
| 1300 | F140W | 281997 | 0.411 | 0.460 | 0.893 |
| 1300 | F110W | 279726 | 0.408 | 0.456 | 0.896 |
| 1350 | F140W | 267978 | 0.412 | 0.460 | 0.895 |
| 1400 | F140W | 223860 | 0.417 | 0.455 | 0.917 |
| 1450 | F140W | 254072 | 0.424 | 0.482 | 0.880 |
| 1500 | F140W | 241233 | 0.435 | 0.488 | 0.892 |
| 1500 | F160W | 233013 | 0.421 | 0.474 | 0.887 |
| 1550 | F160W | 222070 | 0.422 | 0.476 | 0.887 |
| 1600 | F160W | 206349 | 0.433 | 0.505 | 0.857 |
| 1650 | F160W | 176894 | 0.424 | 0.529 | 0.802 |

Table 2: Throughput results for IR11S11A

| wavelength (nm) | filter | observed count rate ($e^-$/sec) | measured throughput | predicted throughput | measured to predicted |
|---|---|---|---|---|---|
| 980 | F098M | 10643 | 0.325 | 0.348 | 0.934 |
| 1050 | F105W | 27430 | 0.356 | 0.377 | 0.946 |
| 1100 | F110W | 39601 | 0.370 | 0.403 | 0.919 |
| 1250 | F125W | 63420 | 0.396 | 0.440 | 0.900 |
| 1258 | F126N | 58362 | 0.356 | 0.406 | 0.879 |
| 1270 | F127M | 63701 | 0.385 | 0.426 | 0.903 |
| 1283 | F128N | 61523 | 0.368 | 0.418 | 0.880 |
| 1301 | F130N | 66980 | 0.397 | 0.447 | 0.888 |
| 1319 | F132N | 63744 | 0.379 | 0.428 | 0.887 |
| 1390 | F139M | 49606 | 0.396 | 0.435 | 0.911 |
| 1400 | F140W | 54884 | 0.408 | 0.455 | 0.897 |
| 1530 | F153M | 53645 | 0.415 | 0.470 | 0.884 |
| 1600 | F160W | 50557 | 0.431 | 0.506 | 0.852 |
| 1645 | F164N | 42764 | 0.414 | 0.518 | 0.798 |
| 1666 | F167N | 38840 | 0.405 | 0.506 | 0.800 |

## Appendix: IR filter blue leaks

The Contract End Item (CEI) specification for out-of-band transmission in the medium-band and wide-band WFC3/IR filters is $10^{-4}$, while for narrow-band filters it is $10^{-5}$ (on average, with no peaks over $10^{-4}$). This level of blocking was not achieved in the IR filter set. In particular, a small wavelength region (~710-830 nm) blueward of the filter bandpass has significantly higher throughput than desired. These blue leaks were considered insignificant when WFC3 included the original IR detector (FPA064), given its low QE below 900 nm. However, these blue leaks became more significant when we switched to thinned IR detectors with better short-wavelength response (e.g., FPA129). The practical scientific impact is minimal and can be calibrated for those rare instances where it might have an impact. For example, observations of an O star in one of the N-band or M-band IR filters could have a few percent of the detected counts coming from flux at these blue wavelengths; thus, the O star would appear a few percent brighter than it would otherwise appear without the blue leaks, but this would not significantly increase the background generated by an O star in a star field. Another pathological situation that could arise would be the redshift of a strong emission line into the blue leak wavelengths (e.g., a high-redshift emission line galaxy). However, in general, blue leaks in IR filters have far less impact than red leaks in UV filters, because most of the universe is red and hot objects are rare. Red leaks in UV filters can cause false detections in surveys of hot objects and can introduce unacceptably high backgrounds when observing hot objects embedded within large populations of cool objects. In contrast, when observing cool objects with IR filters, the contamination from hot objects should be rare, and even in those cases where a hot object is in the vicinity, the small increase in its flux from a few percent blue leak will generally not make the difference between a successful or unsuccessful observation.

We checked the blue leak in this TV campaign by scanning the short wavelength throughput of the 6 IR filters most susceptible to blue leak problems (specifically, those filters that would have the highest fraction of counts coming from blue photons when observing an O star). These tests (IR12S14A & IR12S15) were done in a manner similar to the other throughput tests described in this report, but with a 256x256 subarray on WFC3, and a 10 nm bandpass combined with a lower ND filter on the CASTLE. The OSFLUX values in the headers of these images are not correct, but were corrected after the fact in the analysis here, using new values from the CASTLE operators (R. Telfer, private communication). Because these tests were performed midway throughput the TV campaign, they are subject to the CASTLE instability issue, which can introduce systematic errors at the level of 10-20% in the absolute throughput; however, given the 10 nm bandpass employed in the blue leak tests, the systematic errors are hopefully much smaller. Also, the statistical errors in these measurements are much larger than the nominal throughput tests, because the count rate incident on WFC3 was kept to a relatively small, safe level, to avoid saturation of the detector in the face of uncertain throughput at these wavelengths. Table 3 summarizes the blue leak results for these 6 filters. At most wavelengths, the throughput is at the level of $10^{-6}$, but it can reach as high as $10^{-3}$ to $10^{-2}$ at specific wavelengths

Table 3: Blue leak measurements

| wave-length (nm) | obs. rate ($e^-/s$) | F153W through-put | obs. rate ($e^-/s$) | F164N through-put | obs. rate ($e^-/s$) | F167N through-put | obs. rate ($e^-/s$) | F126N through-put | obs. rate ($e^-/s$) | F128N through-put | obs. rate ($e^-/s$) | F139M through-put |
|---|---|---|---|---|---|---|---|---|---|---|---|---|
| 850 | 99 | 2.52E-06 | 91 | 2.69E-07 | 116 | 3.49E-07 | 96 | 2.85E-07 | 31 | 8.32E-07 | 258 | 7.66E-07 |
| 840 | 108 | 3.38E-06 | 60 | 2.19E-07 | 100 | 3.59E-07 | 60 | 2.21E-07 | 46 | 1.47E-06 | 757 | 2.85E-06 |
| 830 | 126 | 4.66E-06 | 241 | 9.95E-07 | 236 | 1.00E-06 | 52 | 2.33E-07 | 81 | 3.14E-06 | 1079 | 4.83E-06 |
| 820 | 281 | 1.20E-05 | 459 | 2.19E-06 | 501 | 2.39E-06 | 108 | 5.41E-07 | 144 | 7.01E-07 | 1421 | 7.19E-06 |
| 810 | 708 | 3.47E-05 | 865 | 4.83E-06 | 638 | 3.55E-06 | 213 | 1.18E-06 | 154 | 8.48E-07 | 2462 | 1.44E-05 |
| 800 | 14753 | 1.80E-04 | 1689 | 2.13E-05 | 1303 | 1.61E-05 | 635 | 7.90E-06 | 291 | 4.46E-06 | 3082 | 3.84E-05 |
| 790 | 24184 | 3.26E-03 | 336 | 4.63E-05 | 201 | 2.72E-05 | 1176 | 1.60E-04 | 100 | 1.67E-05 | 13863 | 1.87E-03 |
| 780 | 5503 | 7.28E-03 | 475 | 6.42E-04 | 349 | 4.65E-04 | 1462 | 1.93E-03 | 682 | 1.13E-03 | 1996 | 2.63E-03 |
| 770 | 2463 | 2.93E-03 | 1259 | 1.54E-03 | 1319 | 1.57E-03 | 1429 | 1.71E-03 | 1430 | 2.13E-03 | 746 | 8.97E-04 |
| 760 | 9048 | 1.47E-03 | 3472 | 5.74E-04 | 3457 | 5.59E-04 | 5240 | 8.48E-04 | 3231 | 6.44E-04 | 2276 | 3.74E-04 |
| 750 | 10473 | 2.28E-04 | 7645 | 1.72E-04 | 4653 | 1.03E-04 | 8018 | 1.75E-04 | 5151 | 1.42E-04 | 3392 | 7.50E-05 |
| 740 | 3170 | 8.03E-05 | 1647 | 4.29E-05 | 745 | 1.88E-05 | 1187 | 2.98E-05 | 864 | 2.68E-05 | 1171 | 2.99E-05 |
| 730 | 1642 | 1.88E-05 | 1125 | 1.31E-05 | 768 | 8.65E-06 | 874 | 1.13E-05 | 715 | 8.48E-06 | 473 | 5.64E-06 |
| 720 | 4240 | 5.11E-06 | 3908 | 4.82E-06 | 2177 | 2.55E-06 | 1494 | 2.02E-06 | 2247 | 2.81E-06 | 2588 | 3.23E-06 |
| 710 | 1420 | 1.56E-06 | 1283 | 1.43E-06 | 1214 | 1.30E-06 | 1082 | 1.33E-06 | 814 | 9.22E-07 | 760 | 8.65E-07 |
| 700 | 802 | 8.16E-07 | 812 | 8.40E-07 | 635 | 6.34E-07 | 464 | 5.25E-07 | 487 | 5.10E-07 | 520 | 5.43E-07 |